

**Imbricated Aseismic Slip And Fluid Diffusion Drive A Seismic  
Swarm In The Corinth Gulf, Greece.**

Louis De Barros<sup>1,\*</sup>, Frédéric Cappa<sup>1,2</sup>, Anne Deschamps<sup>1</sup>, Pierre Dublanchet<sup>3</sup>

<sup>1</sup> Université Côte d'Azur, CNRS, Observatoire de la Côte d'Azur, IRD, Géoazur, 06560 Sophia Antipolis, France

<sup>2</sup> Institut Universitaire de France, Paris, France

<sup>3</sup> MINES ParisTech, PSL Research University, Centre de Géosciences, 35 rue Saint-Honoré 77305 Fontainebleau, France

\* Corresponding author: [debarros@geoazur.unice.fr](mailto:debarros@geoazur.unice.fr) (L. De Barros)

**Contents of this file**

Figures S1 to S6

Text S1 to S2

**Additional Supporting Information (Files uploaded separately)**

Caption for supplementary movie S1

**Introduction**

The supporting information includes one movie, two texts and six figures:

- Movie S1 shows the location of the events through time.
- Text S1 describes the detection process using the small aperture antenna.
- Figure S1 is a set of nine cross-sections that slice the seismic clouds.
- Figure S2 shows the depths of the hypocenters versus time of occurrence.
- Figure S3 shows an example of waveforms of a family of 10 repeaters.

- Figure S4 shows the locations of the repeaters.
- Figure S5 compares the time distribution of the repeaters with the time distribution of all the seismicity in the exact same periods.
- Text S2 theoretically links the migration velocity to the slip velocity.
- Figure S6 shows the slip velocity as a function of migration velocity and stress drop.

## References

Ampuero, J.-P., and A. M. Rubin (2008), Earthquake nucleation on rate and state faults: Aging and slip laws, *J. Geophys. Res.*, 113, B01302, doi:10.1029/2007JB005082.

Cansi, Y., 1995. An automatic seismic event processing for detection and location: The P.M.C.C. Method. *Geophys. Res. Lett.* 22, 1021–1024.

Gao, H., Schmidt, D.A., Weldon, R.J., 2012. Scaling Relationships of Source Parameters for Slow Slip Events. *Bull. Seismol. Soc. Am.* 102, 352–360.

Lohman, R.B., and McGuire, J.J. (2007), Earthquake swarms driven by aseismic creep in the Salton Trough, California. *J. Geophys. Res.*, 112, B04405, doi:10.1029/2006JB004596.

Roland, E., and McGuire, J.J. (2009), Earthquake swarms on transform faults, *Geophysical Journal International*, 178, 1677–1690, doi: 10.1111/j.1365-246X.2009.04214.x

Rost, S., Thomas, C., 2002. Array seismology: Methods and applications. *Rev. Geophys.* 40 (2), 1-27.

Rubin, A. M. (2008), Episodic slow slip events and rate-and-state friction, *J. Geophys. Res.*, 113, B11414, doi:10.1029/2008JB005642.

**Movie S1.** Movie of the event locations through time in a 3D view from South, between days 272 and 280. Empty circles are for past events, while filled circles shown the events within a 2.4 hours windows around the given time. Colors shown the elapsed time and the circles are sized by the magnitude of the events.

### **Text S1: Detection process using the small aperture antenna**

To improve the detection level, we use a nearby antenna of 7 stations (MG, Fig. 1) and we look for spatially correlated signals (De Barros et al., 2017). The small aperture (less than 500 m) of this mini-array allows the events to share similar waveforms at the 7 stations. To perform the detection, we use the following steps (Cansi, 1995; Rost and Thomas, 2002):

- 1- The data are filtered in a 2-8 Hz frequency band.
- 2- Cross-correlation functions between all pairs of stations are computed for 4-seconds long sliding windows, with one second overlap.
- 3- The maximum of all correlation functions are averaged among all pairs of stations. If this mean correlation coefficient is above 0.6, a possible event is detected. Subsequent time windows with correlation coefficient above 0.6 are assumed to be part of the same detection.
- 4- For the detected events, a back-azimuth is computed. Delay times between pairs of stations are measured from the correlation functions. They are then inverted to determine the back-azimuth under a plane-wave approximation (Rost and Thomas, 2002).
- 5- If the back-azimuth lies between  $210$  and  $290^\circ$  (i.e. the mean azimuth to the swarm  $\pm 40^\circ$ ), the detected waveforms are selected as seismic events, possibly originated from the swarm.

Despite a smaller number of detected events than using a template matching approach, such method has the advantage of being more exhaustive, as it is not dependent on template choices, and can therefore detect unconventional seismicity such as tremors, if any.

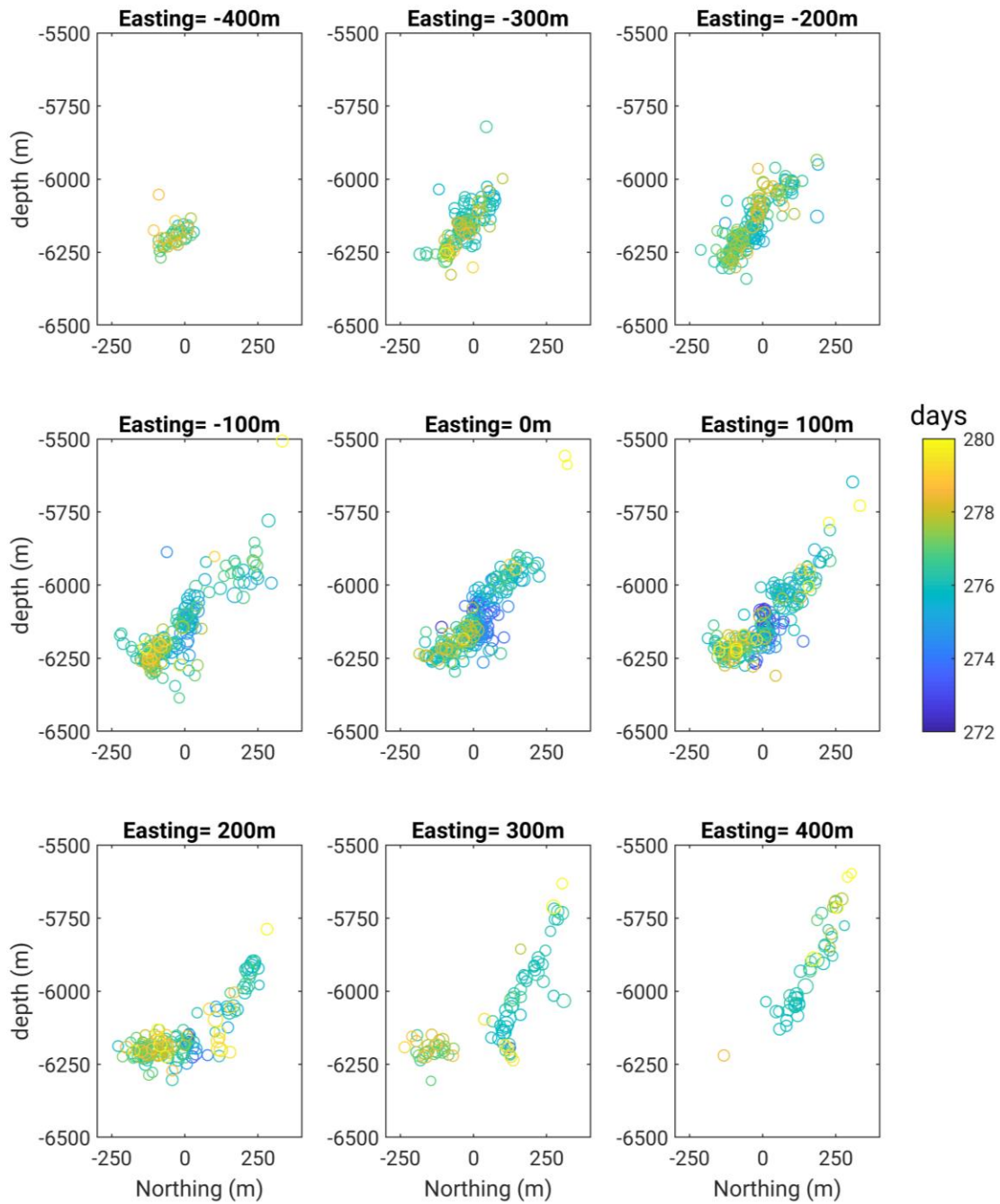


**Figure S1.** South-North cross-sections, centered every 100 m at Easting between -400 m and 400 m, with events in a +/- 50 m Easting range around this center. The color code shows the day of occurrence in 2015.

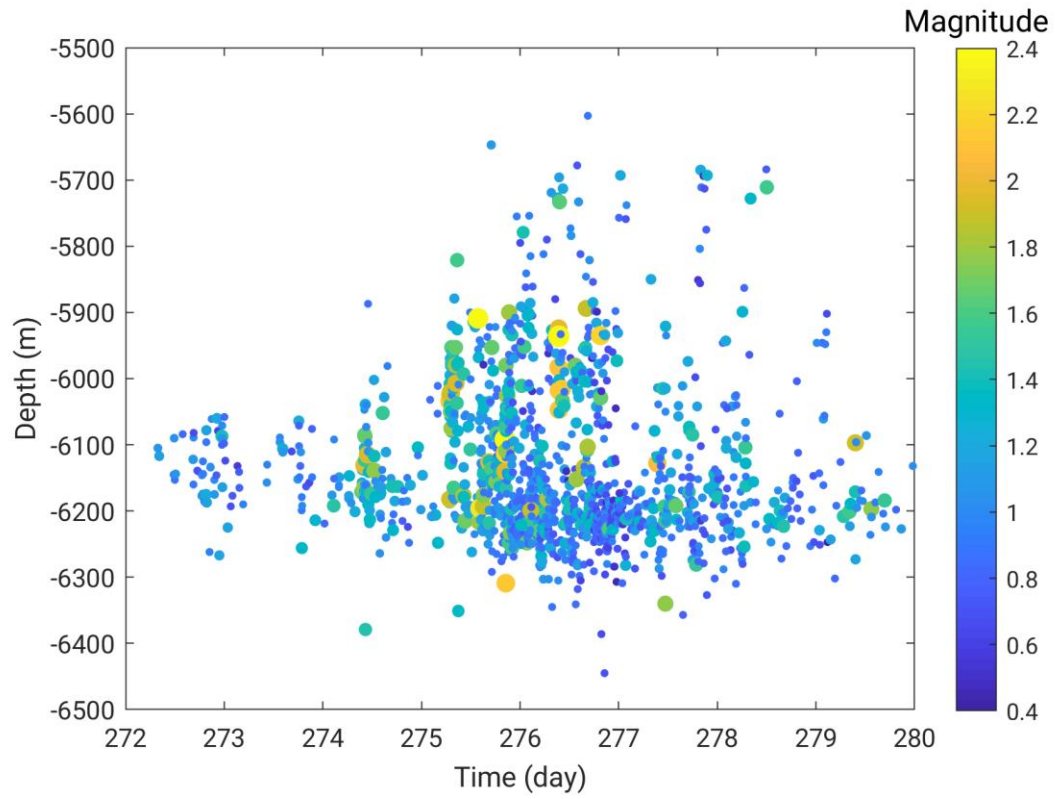


**Figure S2.** Depths of the hypocenters versus days of occurrence. The colors show the magnitude of the events.

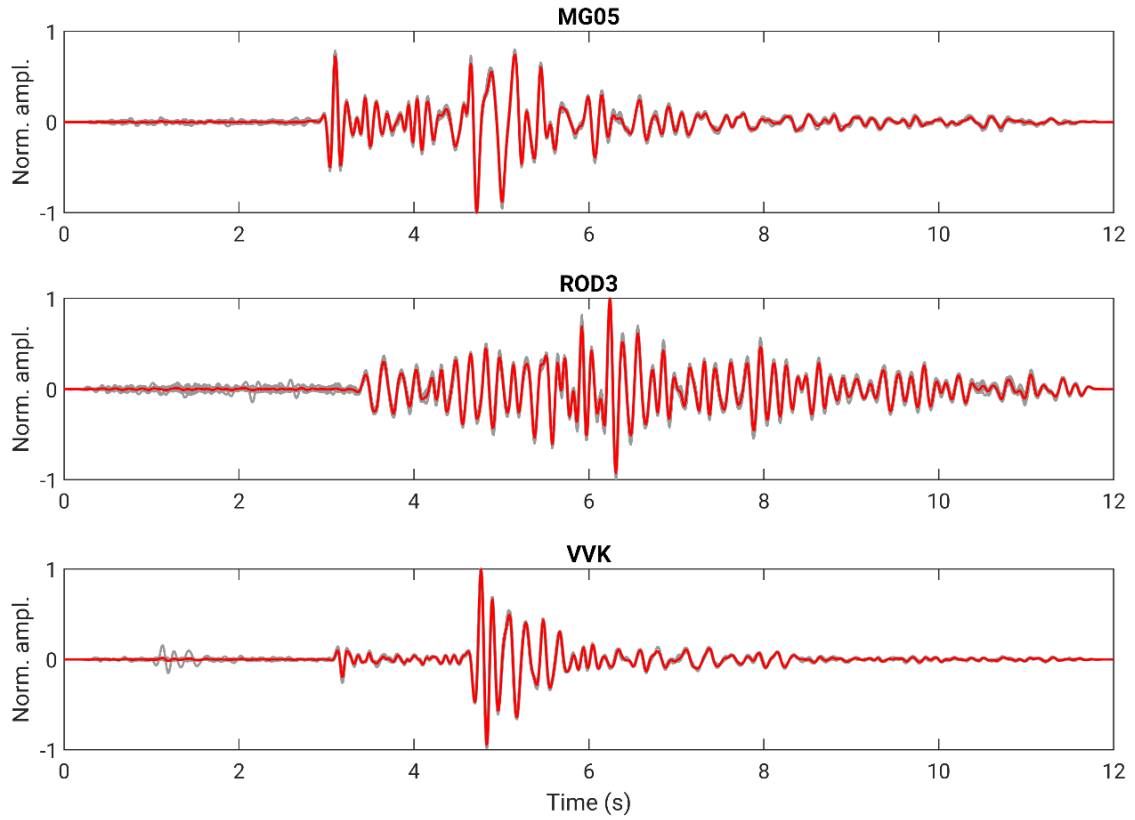


**Figure S3.** Examples of a repeater family of 10 events, recorded at three stations (MG, ROD3 and VVK). In each panel, normalized waveforms of the 10 events are shown in gray, with the stack waveforms in red.

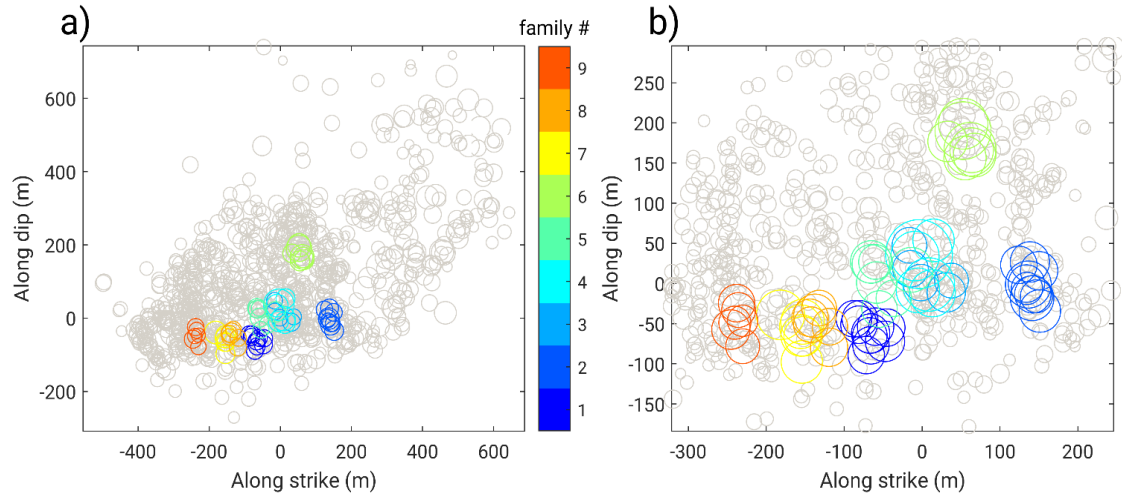


**Figure S4.** Location of the repeating events. (a) View of the full seismic swarm, projected onto the main structure. (b) Zoom on the area where the repeating events are located. In both panels, repeating events are colored according to their family and are sized according to their source size. Gray circles indicate events with lower correlation coefficient.

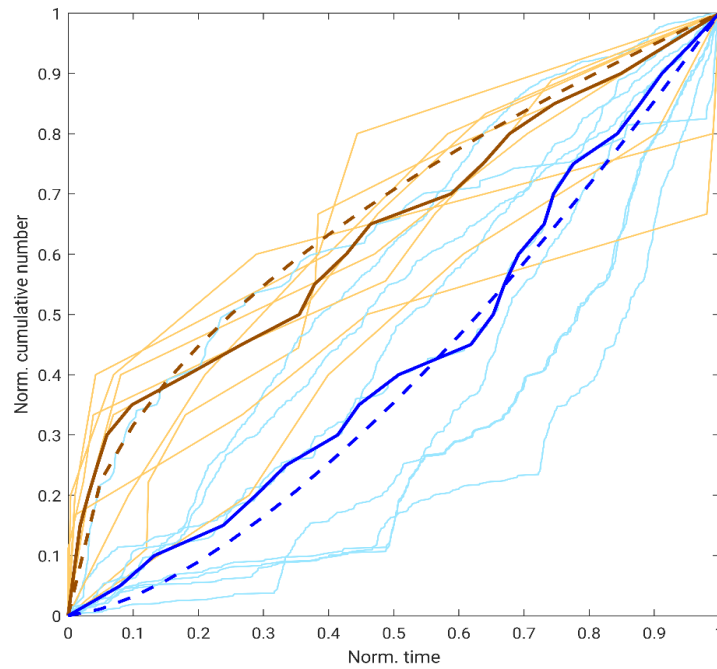


**Figure S5.** Cumulative number of events versus time for multiplet families (orange lines). The cumulative number of located events in the exact same times of the multiplet families is shown for reference (light blue). Both cumulative number of events and time are normalized to make them comparable among all families. The average cumulative number of events for the multiplet families and the located events are shown as thick brown and blue lines, respectively. They can be fitted (dashed lines) by relation of the form  $N \sim t^\alpha$ , with  $\alpha=0.5$  and  $\alpha=1.5$  for the multiplet and located events, respectively.

## Text S2: Rupture migration velocity and slip velocity

Ampuero and Rubin (2008), and Rubin (2008) showed that the velocity of a rupture front propagating with a quasi-steady shape is well approximated by:

$$v_r = \frac{\mu \cdot v_{max}}{\Delta\sigma} \quad (1)$$

where  $v_{max}$  is the maximum slip velocity,  $\Delta\sigma$  is the stress drop,  $\mu$  is the shear modulus. Based on the rupture migration velocity estimated during the rapid bursts of seismicity (2 to 10 km/day, Figs. 3a-b in the main text), a rock shear modulus of 30 GPa, and a range of reasonable stress drop for a seismic swarm (0.01 to 1 MPa), we can estimate a range of fault slip velocity using equation 1.

Figure S5 indicates that the fault slip velocity at the maximum earthquakes rupture migration velocity (10 km/day) observed during the swarm varies between  $0.5$  and  $3.86 \times 10^{-6}$  m/s over a range of stress drop comprised between 0.01 and 1 MPa (Gao et al., 2012). This range of values of slip velocity is consistent with previous studies of seismic swarms driven by aseismic slip transients (Lohman and McGuire, 2007; Roland and McGuire, 2009).

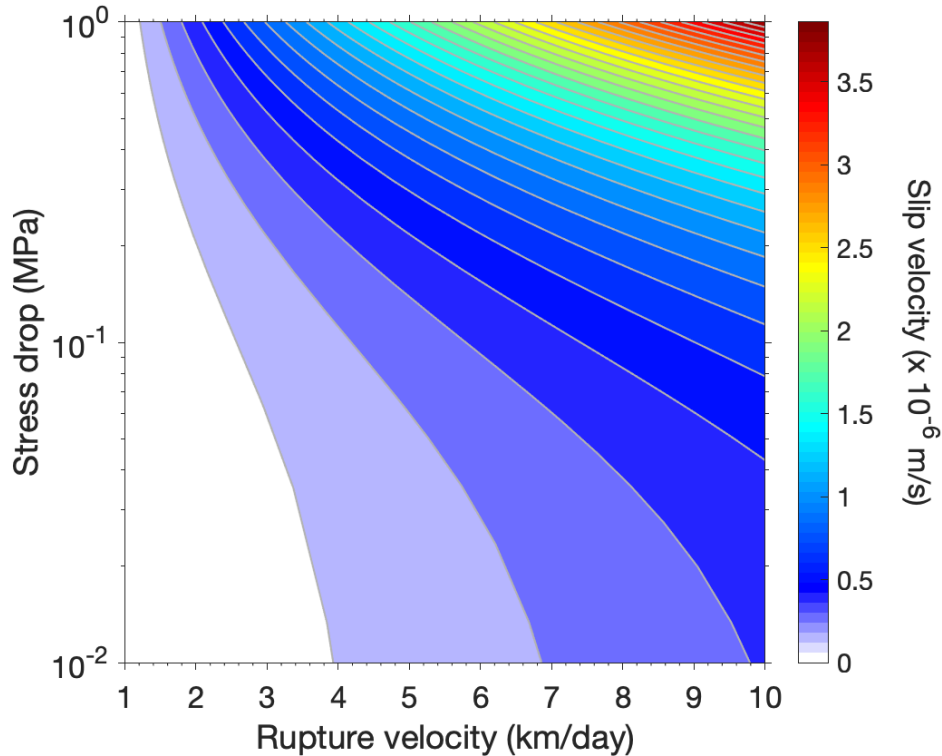


**Figure S6.** Fault slip velocity estimated from the observed rupture migration velocity during rapid bursts of seismicity and a range of plausible stress drop during the seismic swarm. The maximum slip velocity is estimated at  $3.86 \times 10^{-6}$  m/s for a stress drop of 1 MPa and a rupture velocity of 10 km/day.